

US Department of Energy National Lab Activities in Marine Hydrokinetics: Machine Performance Testing

V.S. Neary^{1, 2}, L.P. Chamorro², C. Hill², B. Gunawan¹, F. Sotiropoulos²

¹ Oak Ridge National Laboratory,
1 Bethel Valley Road,
P.O. Box 2008, MS 6036, Oak Ridge, Tennessee, 37831, U.S.A.
E-mail: nearyvs@ornl.gov

² St. Anthony Falls Laboratory,
University of Minnesota,
2 Third Avenue S.E., Minneapolis, Minnesota, 55414, U.S.A.

Abstract

Marine and hydrokinetic (MHK) technology performance testing in the laboratory and field supports the US Department of Energy's MHK program goals to advance the technology readiness levels of MHK machines, to ensure environmentally responsible designs, to identify key cost drivers, and to reduce the cost of energy of MHK technologies. Laboratory testing results from scaled model machine testing at the University of Minnesota's St. Anthony Falls Laboratory (SAFL) main channel flume are presented, including simultaneous machine power and inflow measurements for a 1:10 scale three-bladed axial flow turbine used to assess machine performance in turbulent flows, and detailed measurements of inflow and wake flow velocity and turbulence, including the assessment of the effects of large energetic organized vortex shedding on machine performance and wake turbulence downstream. Scaled laboratory testing provides accurate data sets for near- and far-field hydrodynamic models, and useful information on technology and environmental readiness levels before full-scale testing and demonstration in open water. This study validated turbine performance for a technology in order to advance its technology readiness level. Synchronized ADV measurements to calculate spatio-temporal characteristics of turbulence supported model development of the inflow turbulence model, Hydro-TurbSim. Wake flow measurements supported model development of the far-field model, SNL-EFDC to optimize spacing for MHK machine arrays.

Keywords: Turbulence, ADV, autospectra, wake recovery

1. Introduction

Understanding the interaction between turbulent flow and hydrokinetic energy conversion devices is important in order to advance marine and hydrokinetic (MHK) technologies to commercialization. Increased turbulence levels and their asymmetries over the energy extraction plane affect the hydrodynamic loads on the MHK device and its performance. The effects of increased turbulence from various sources, including upstream hydrokinetic devices, in-stream structures and moving vessels, are of particular concern when the frequencies of turbulence may correspond closely to natural frequencies of the device components or the rotation frequency of the blades. The MHK device also has pronounced effects on the turbulent flow field, especially in the wake of the device where pressure and velocity is reduced, turbulence levels increase and vortices are generated and shed downstream from the tower and blades. These effects are investigated in the St. Anthony Falls Laboratory flume by measuring instantaneous velocities along profiles and points around a 1:10 scale MHK axial-flow turbine using a synchronized acoustic Doppler velocimeter (ADV) array and an acoustic Doppler profiler (ADP). Profiles of velocity and Reynolds stresses are presented to show the effects of the device on the flow field and the wake recovery distance. Spectral energy density plots of inflow turbulence and turbine power, which are simultaneously measured, allow insight into the effects of turbulence on the turbine performance.

Scaled model studies of marine and hydrokinetic (MHK) technologies, including current energy converters, e.g. water turbines, allow detailed flow field measurements around the device, while simultaneously collecting information on turbine loading and performance. Dimensional analysis provides scaling laws that are used to upscale model test information

into performance and design information for a full-scale prototype turbine. For water turbines, hydrodynamic similarity is achieved when the chord Reynolds number (Re_c), Froude number (Fr), and the tip speed ratio (λ) of the model and the full-scale device are the same. It is rare to achieve perfect similarity for Re_c , but a threshold value should be exceeded, or boundary layer trips should be employed, to ensure the flow is fully turbulent and simulates the essential physics of flow-machine interaction. Froude number similarity in open channel testing is usually met and is particularly important for upscaling wake flow data.

The study objectives were to: 1) Develop a performance curve for a scaled model axial flow turbine; 2) Collect and process turbulent flow measurements that can be used for inflow boundary conditions (including effects of energetic vortex shedding) to inform turbulent inflow models and machine design codes; and 3) Examine inflow and wake flow hydrodynamics, and turbine response to turbulence, for a scaled turbine in a large open channel flume (including effects of energetic vortex shedding).

2. Methods

Our research was conducted at the St. Anthony Falls Laboratory (SAFL) Main Channel facility shown in Figure 1. The SAFL Main Channel is 2.8 m wide, 1.8 m deep, and 85 m long with a maximum flow discharge of 8.5 m³/s. The discharge rate is monitored using a Massa ultrasonic range sensor mounted upstream of the sharp-crested weir tailgate. A 1:10 scale axial flow turbine was mounted to the floor in the center of the channel approximately 40 m (80 diameters) downstream of flow straighteners. For these experiments, the discharge (Q), depth (h) and bulk velocity (U_b) were 1.265 m³/s, 1.15 m and 0.4 m/s respectively. The SAFL Main Channel Data Acquisition (DAQ) Carriage, capable of completing longitudinal, lateral, and vertical travel within 1 mm accuracy, was utilized to position instruments for data acquisition.



Figure 1. SAFL Main Channel and DAQ carriage looking upstream.

The model turbine shown in Fig. 2 (top) was a 1:10 scale axial flow turbine with a diameter (d) of 0.5 m. It was equipped with an instrumentation package developed by SAFL engineers to measure turbine power output via measurements of angular velocity and torque at 200 Hz. An Interface MRT-2NM torque transducer and a Pacific Scientific M21 Powermax II stepper motor were housed in the upstream cone of the turbine nacelle. The stepper motor was affixed to the turbine nacelle by way of the torque transducer and “floated” in the instrumentation chamber located in the nacelle nose cone. Additionally, a thermocouple was connected to the stepper motor to monitor operating temperatures. All wires were routed through the turbine tower, through vinyl tubing connected to the floor of the SAFL Main Channel, and out to the control computer. A feedback algorithm allowed precise control of angular velocity for the turbine by setting the rotational speed of the stepper motor (Figure 2.7). The software recorded torque measurements; typically at 200 Hz. Temperature was recorded at the beginning and end of each data file to monitor drift in the operating temperature; however, little drift was ever observed in the data. See more details in [2].

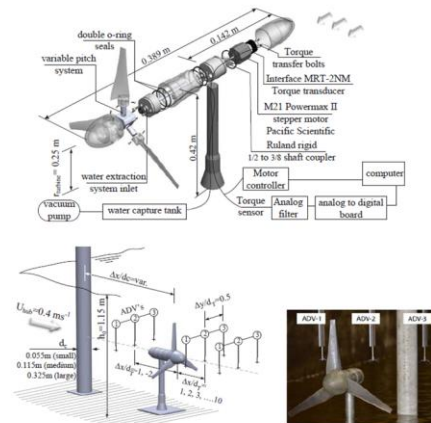


Figure 2. Top: Exploded diagram of the model hydrokinetic turbine construction including the instrumentation package installed in the nacelle of the turbine (from [2] Chamorro et al, 2012). Bottom: Experimental set-up. Turbine, cylinder, ADV array and measurement locations (left); photograph of the turbine and cylinder partially submerged with the ADV array (right).

Instantaneous three-component velocity measurements were collected using Oak Ridge National Laboratory’s (ORNL) 3-synchronized Nortek Vectrino ADV array (Fig. 2, bottom), and SAFL’s Sontek pulse-coherent acoustic Doppler profiler (PC-ADP). Multiple points and instantaneous vertical velocity profile measurements around the model turbine were collected. The ADV measurement grid is shown in Fig. 2 (bottom left). Mean flow statistics were determined along the centerline plane and vertical planes aligned with the rotor hubs at $x/d = -10, -5, -3, -2, 1, 2, 3, 4, 5, 6, 7, 8, 9, 10, 11, 12, 13, 14, 15, 16, 17, 18, 19, 20, 25, 30,$ and 35 , where $x/d = 0$ corresponds with the rotor plane of the turbine. The ADV array was

used to collect high resolution vertical profiles of instantaneous velocity from 1 to 10 rotor diameters downstream of the turbine rotor plane, and from 1 to 3 diameters upstream. Vertical profiles were measured at 30 to 40 sample locations. An additional vertical profile was collected 5 to 10 diameters upstream to document the nearly-fully developed flow entering the turbine test section. Lower resolution velocity profiles were measured beyond 10 diameters downstream using the ADP.

Torque time series data at 200 Hz, as illustrated in Fig. 3, were collected at each angular velocity setting for 5 minutes. The high-resolution torque measurements allowed for time-resolved fluctuations of turbine power output, and for a detailed examination of the turbine response to approach flow turbulence characteristics. Instantaneous turbine power output was calculated as,

$$P_t = \omega \cdot \tau$$

where P_t is instantaneous turbine power, ω is the instantaneous angular velocity, and τ is the instantaneous torque at each tip speed ratio. Using these computed turbine power outputs at each tip speed ratio, we calculated the instantaneous power coefficient (C_p) as,

$$C_p = \frac{P_t}{P_a} = \frac{2P_t}{\rho A u^3}$$

where P_a is the available hydrokinetic power of the approach flow, ρ is the fluid density, A is the blade swept area, or area of the energy extraction plane (EEP), and u is the instantaneous free stream velocity of the approach flow measured simultaneously at the hub centerline of the turbine rotor, and the centroid of the EEP for each river turbine rotor. The mean values for P_t , P_a , and C_p , were calculated for each test case.

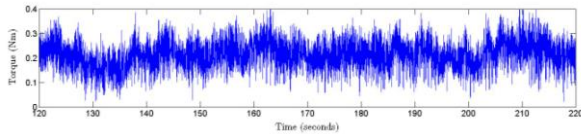


Figure 3. Sample time-series plot of 200-Hz torque measurements.

Periodic and coherent energetic motions were introduced in the flow by placing a cylinder upstream and in the symmetry plane of the turbine. Cylinder diameters of $d_c = 0.055$, 0.115 and 0.325 m (hereon referred to as a small, medium and large cylinder, respectively) were considered. Each of these induced von Karman vortices characterized by Strouhal numbers $S = f_v d_c / U$ of 0.2, where, f_v is the von Karman shedding frequency, d_c is the cylinder diameter, U is the mean flow velocity and $Re = U d_c / \nu$ is the Reynolds number. The respective von Karman shedding frequencies were 0.24, 0.69 and 1.44 Hz for the large, medium and small cylinders. These three frequencies

were selected to be in the responsive region of the turbine [2], where the diameter of the small cylinder produced a shedding frequency similar to the turbine frequency ($f_T = 1.5$). Each cylinder was placed at three locations. The small and medium cylinders were placed at $x/d_c = -7.5$, -10 , and -15 , while the large cylinder was located at $x/d_c = -3$, -6 , and -8 . Ten scenarios were studied: three cases for each cylinder, which were compared with the case without the cylinder.

3. Results

The performance curve, C_p , vs. tip-speed-ratio (λ) is shown in Fig. 4. Tabulated results are summarized in Table 1. The performance study advanced the technology readiness level of the axial flow turbine design by documenting the turbine performance characteristics and identifying the conditions for optimal performance, with a maximum power coefficient $C_p = 0.47$ occurring at $\lambda = 5$.

RPM	Tip Speed Ratio	Mean Torque	C_p
30	1.9	0.1601	0.0743
45	2.9	0.3010	0.2096
60	3.9	0.3836	0.3562
75	4.9	0.4015	0.4660
85	5.6	0.3523	0.4634
90	5.9	0.3456	0.4813
105	6.9	0.2442	0.3968
120	7.8	0.1120	0.2080
135	8.8	-0.0260	-0.0544

Table 1: Settings used for developing the performance curve of the horizontal axis hydrokinetic turbine.

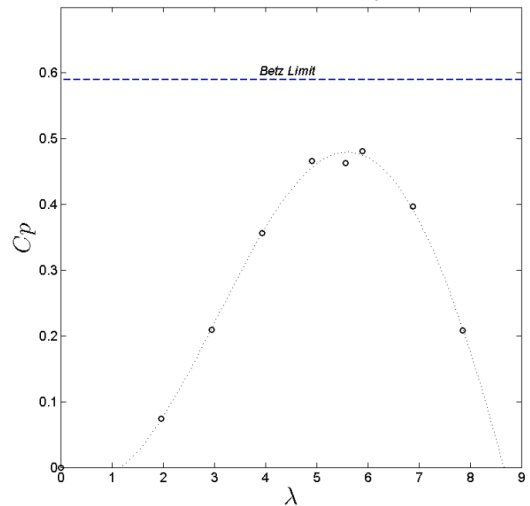


Figure 4. Performance curve relating C_p vs. tip speed ratio (λ).

Wake recovery was examined for the optimal power coefficient case by plotting the mean velocity deficit measured at the centerline of the rotor downstream of the rotor plane at $x/d_T = 0$, as shown in Fig. 5. The flow

recovers rapidly to a mean velocity deficit of about 0.35 at $x/d_T = 6$. The recovery rate beyond this point is relatively slow by comparison. Introducing coherent energetic vortex shedding with the small cylinder upstream is found to accelerate recovery by increasing mixing of the free stream and the wake flows. The same effect was found for the medium and small cylinders. Proximity of the cylinder to the turbine was found to have a measurable, albeit modest, effect on the recovery rate.

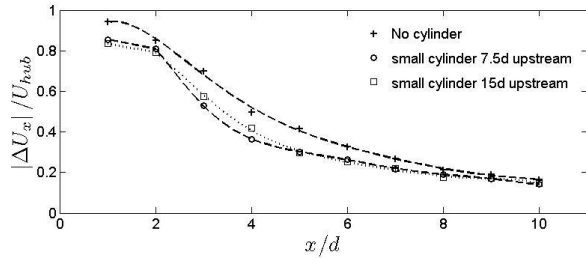


Figure 5. Mean velocity deficit in the center of the wake at hub height.

The impact of the flow turbulence on turbine power fluctuations was examined by plotting the spectra of the approach flow in the symmetry plane of the turbine at hub height and one rotor diameter upstream, as shown in Fig. 6a. The cylinder was found to modify the structure of the approach flow through a broad frequency range $f \in [0.06 \text{ } 0.7] \text{ Hz}$. The shedding frequency associated with this cylinder and flow condition was within this range ($f_K \approx 0.24$). The corresponding spectra of the turbine power for these two scenarios are depicted in Fig. 6b. This plot illustrates the effect of the 'added' turbulence on the turbine power. The spectral structure of the turbine power was modified essentially in the same frequency range where the cylinder alters the turbulent structure of the flow. A similar phenomenon was observed when the cylinder was placed at $x/d_c = -3$ and -8 and for the medium cylinder (results not shown here).

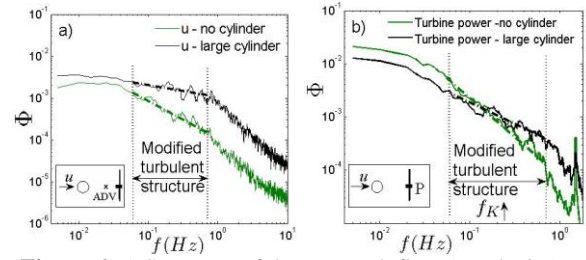


Figure 6. a) Spectrum of the approach flow (u -velocity) at one rotor diameter upstream of the turbine; b) Spectrum of the turbine power. Large cylinder ($d_c = 0.325 \text{ m}$, $x/d_c = -6$). From [1].

4. Conclusions

Laboratory testing results from scaled model machine testing at the University of Minnesota's St. Anthony Falls Laboratory (SAFL) main channel flume provide valuable insights on how turbulence affects turbine power response and wake flow dynamics. Large coherent energetic motions have a pronounced influence on these phenomena and deserve more attention because they can occur at hydrokinetic energy sites as a result of obstacles, e.g. bridge piers, and upstream turbines with arrays. While the interaction between approach flow turbulence and turbine power response is complex, with a broad range of turbulence scales at work, studies of coherent energetic motions with well-defined shedding frequencies can provide valuable insights into this problem.

Acknowledgements

This research was supported by the U.S. Department of Energy's (DOE) Office of Energy Efficiency and Renewable Energy, Wind and Water Power Technologies Program. Oak Ridge National Laboratory is managed by UT-Battelle, LLC for DOE under contract DE-AC05-00OR22725.

References

- [1] L.P. Chamorro, V.S. Neary, C. Hill, B. Gunawan, R. Arndt, F. Sotiropoulos. (2012): Effect of energetic coherent motions on the power and wake of an axial-flow turbine. Submitted to J. of Fluid Mech.
- [2] L.P. Chamorro, Hill, C., Morton, S., Ellis, C., Arndt, R.E.A., and Sotiropoulos, F. (2012): On the interaction between a turbulent open channel flow and an axial-flow turbine. Submitted to J. of Fluid Mech.